Discovery of Three 22-Membered Macrolides by Deciphering the Streamlined Genome of Mangrove-Derived *Streptomyces* sp. HM190

Yanghui Ye[1], Nusratgul Anwar[2], Xuming Mao[2], Shihua Wu[2], Cen Yan[1], Zhe Zhao[2], Ran Zhang[2], Yanfang Nie[2], Jianwei Zhang[3], Jidong Wang[4]* and Min Wu[1]*

[1] Ocean College, Zhejiang University, Hangzhou, China, [2] College of Life Sciences, Zhejiang University, Hangzhou, China, [3] Cardiovascular Health Department, AstraZeneca Trading Co., Ltd., Wuxi, China, [4] Key Laboratory of Vector Biology and Pathogen Control of Zhejiang Province, College of Life Science, Huzhou University, Huzhou, China

Strain HM190, a moderate halophile, was isolated from rhizosphere soil of the mangrove *Kandelia obovata* in Fugong village, China. The 16S ribosomal RNA (rRNA) gene sequence and the results of phylogenetic analysis revealed that strain HM190 belonged to the genus *Streptomyces* and had the highest sequence similarity of 99.79% to *Streptomyces heilongjiangensis* NEAU-W2$^{\text{T}}$. The complete genome of strain HM190 comprised 7,762,826 bp in a linear chromosome with 71.97% G + C content. According to antiSMASH analysis, a total of 30 biosynthetic gene clusters (BGCs) were predicted to be involved in secondary metabolism, 12 of which were responsible for the production of polyketide- and non-ribosomal peptide-derived secondary metabolites. Gene cluster 5 was responsible for macrolide biosynthesis in a strain-specific 126,331-bp genomic island belonging to the left-arm region. Combined genomics–metabolomics analysis led to the discovery of three 22-membered macrolides (compounds **1–3**). Their structures were elucidated by using spectroscopic techniques including high-resolution electrospray ionization mass spectroscopy (HRESIMS) and nuclear magnetic resonance (NMR). The absolute configurations of compounds **1–3** were determined by the X-ray single crystal diffraction and NMR data analysis. All three compounds displayed moderate cytotoxic activities toward tumor cell lines HepG2, A549, and HCT116.

Keywords: *Streptomyces* sp. HM190, biosynthetic gene clusters, 22-membered macrolides, structure elucidation, cytotoxic activities

INTRODUCTION

Mangrove ecosystems cover about 60–75% of the world's tropical and subtropical coastlines and grow in saline coastal sediment habitats at transition zones with ocean, fresh water, and land (Holguin et al., 2001). The tidal action in these areas causes large changes in temperature, oxygen, and salinity levels during the day, which leads to the formation of unique microbial communities (Kathiresan and Bingham, 2001). The phylogenetic diversity of mangrove microbial communities

has been well established based on 16S ribosomal RNA (rRNA) analytical approaches, including PCR cloning (Li et al., 2011), denaturing gradient gel electrophoresis (Tian et al., 2008), and pyrosequencing (Santos et al., 2011). Recently, various mangrove-derived microorganisms have attracted increasing attention in the drug discovery field, especially those of the genus *Streptomyces*, as important sources of biologically active compounds with diverse structures (Xu, 2011; Thatoi et al., 2013; Blunt et al., 2015).

The genus *Streptomyces* belongs to the family *Streptomycetaceae*, the order *Streptomycetales*, and the class *Actinobacteria*, and was originally described in Waksman and Henrici (1943). At the time of writing, 854 *Streptomyces* species with validly published names had been proposed according to List of Prokaryotic names with Standing in Nomenclature[1]. Some of these *Streptomyces* strains have been isolated from a wide range of marine habitats, including mangroves (Yan et al., 2010), marine sediments (Zhao et al., 2009), seawater (Zhu et al., 2011), sponges (Huang et al., 2016), algae (Girão et al., 2019), and corals (Alfredo et al., 2017). *Streptomyces* constitutes an important source of new natural products because its strains contain a large number of biosynthetic gene clusters (BGCs) associated with the production of multiple secondary metabolites (Hwang et al., 2014; Liu et al., 2018). Since the first complete genome of *Streptomyces coelicolor* A3(2) was sequenced and reported in Bentley et al. (2002), increasing numbers of *Streptomyces* genomes have been sequenced and deposited in public databases in recent years (Studholme, 2016), which has led to an increase in genomics–metabolomics studies of this genus (Xu et al., 2019). However, most of these genomes were draft genomes. The number of complete genomes of *Streptomyces* has been limited because of their high G + C content, which results in shorter reads and much higher error rates during genome sequencing (Ioanna et al., 2012; Zhong et al., 2013).

During our work focused on discovering microorganism diversity from mangrove sample, Strain HM190, as a novel species of the genus *Streptomyces*, was isolated from rhizosphere soil of the mangrove *Kandelia obovata* in Fugong village, Zhangzhou, China. The complete genome of the strain was sequenced, and 30 gene clusters were predicted to be involved in the biosynthesis of secondary metabolites using the antiSMASH 5.0 software (Blin et al., 2019). Genome analysis of the isolate indicated that gene cluster 5 was probably involved in the production of a compound structurally similar to the macrolide of apoptolidin, based on its high similarity to the type I polyketide synthase (PKS) from the apoptolidin BGC of *Nocardiopsis* sp. FU 40 (Du et al., 2011). As a result, three 22-membered macrolides (compounds **1**–**3**, **Figure 1**) were isolated from its fermentation broth. The absolute configuration of compound **1** was confirmed by X-ray single-crystal diffraction. The absolute configurations of compounds **2** and **3** were established through detailed nuclear magnetic resonance (NMR) data analysis in comparison with compound **1** and other related compounds. Herein, we describe the isolation, structure elucidation, and cytotoxic activity of the three compounds.

---

[1]http://www.bacterio.net/streptomyces.html

MATERIALS AND METHODS

General Experimental Procedures

Silica gel plates HSGF254 (Yantai Chemical Industry Research Institute, Yantai, China) were used for thin-layer chromatography (TLC). Column chromatography was performed with commercial silica gel (QingDao HaiYang Chemical Group Co., QingDao, China, 200-300 mesh). High-performance liquid chromatography (HPLC) separation was performed on semipreparative HPLC (Agilent 1100, Zorbax SB-C18, 5 μm, 250 × 9.4 mm inner diameter; 1.5 mL/min; 210 nm; Agilent, Palo Alto, CA, United States). NMR spectra were measured with a Bruker DRX-400 spectrometer (Bruker, Rheinstetten, Germany). The HRESIMS spectra were taken on a Q-TOF Micro LC-MS-MS mass spectrometer (Waters Co., Milford, MA, United States). Optical rotation was measured on a Perkin-Elmer 341 polarimeter (Perkin-Elmer, Suzhou, China). IR spectra were recorded on a Nicolet Magna FT-IR 750 spectrometer (Nicolet, Tokyo, Japan). UV spectra were recorded on a Varian CARY 300 BIO spectrophotometer (Varian, Cary, NC, United States).

Isolation and Identification of Strain HM190

Strain HM190 was isolated from a soil sample collected from rhizosphere soil of the mangrove *K. obovata* of Fugong village (117° 57′ N 24° 24′ E), in Zhangzhou, China, which was placed into clean plastic buckets and stored at 4°C until use. Serially diluted (10-fold dilutions each) samples were made and spread on the five selective isolation media by the traditional dilution-plating method: HV (humic acid-vitamin agar medium), M7 (glycerine-peptone agar medium), GS (Gauze's modified medium no. 1), ISP2 (ISP medium no. 2), and MA (marine agar 2216 medium). All of the media were supplemented with 25 mg/L of nalidixic acid and 50 mg/L of nystatin. After 7 days of incubation at 30°C, a white-pigmented colony was picked from MA plates and named as HM190. After repeated plate streaking on the same medium, pure strains were obtained from individual colonies and preserved at −80°C as suspension with 25% (v/v) glycerol for further use (Ye et al., 2019).

For phylogenetic studies, the isolate was grown in MB (marine broth 2216 medium) for 7 days at 30°C. The 16S rRNA gene sequence amplification was performed by using universal primers 27F [5′-AGAGTTTGATCCTGGCTCAG-3′] and 1492R [5′-ACGGCTACCTTGTTACGACTT-3′] (Anzai et al., 2000). Amplification reactions were prepared in a 25 μL final reaction volume containing 12.5 μL of PCR SuperMix, 11 μL of distilled water, 0.5 μL of each primer, and 0.5 μL of extracted DNA template. PCR was performed under the following conditions: 30 cycles of 94°C/5 min, 4°C/30 s, 55°C/30 s, 72°C/75 s and a final extension of 72°C/10 min. PCR products were ligated to vector pMD 19-T (TaKaRa) and cloned into *Escherichia coli* DH5a for sequencing, and the almost-complete sequence of the 16S rRNA gene sequence was obtained. The obtained sequence was assembled with DNASTAR SeqMan (LaserGene, Madison, WI, United States). Further, the 16S rRNA gene

FIGURE 1 | Structures of compounds **1–3**.
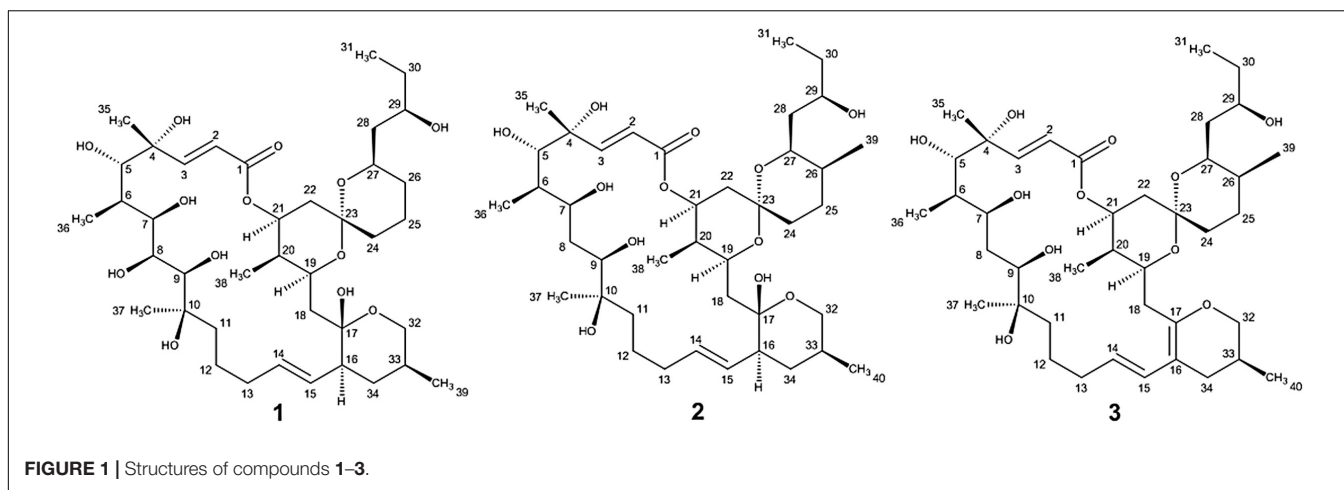
sequence was analyzed by submitting to the NCBI[2] and the EzTaxon-e server[3] (Altschul et al., 1997; Yoon et al., 2017). The multiple sequences were aligned with Clustal W (Thompson et al., 1994). Phylogenetic trees were constructed with the MEGA 5.0 software package (Molecular Evolutionary Genetics Analysis, version 5.0) (Tamura et al., 2011) by using neighbor-joining (Saitou and Nei, 1987), minimum-evolution (Rzhetsky and Nei, 1992), and maximum-likelihood (Felsenstein, 1981). Bootstrap analysis (1000 replicates) was used to evaluate the trees topology. Kimura two-parameter model was used for phylogeny construction and evolutionary distances analysis (Kimura, 1981). The GenBank/EMBL/DDBJ accession number for the 16S rRNA gene sequence of strain HM190 is MN897722.

Genome Sequencing and Annotation

For DNA isolation, strain HM190 was inoculated into MB medium and grown at 30°C with shaking (200 r/min) for 7 days. High-quality genomic DNA was extracted using the Bacteria Genomic DNA Extraction Kit (DongSheng Biotech) according to the manufacturer's instructions. The genome was sequenced using the PacBio RS II platform and the Illumina HiSeq 4000 platform (Beijing Genomics Institute) (163-fold). Four SMRT cells Zero-Mode Wave guide arrays of sequencing were used by the PacBio platform to generate the sub-reads set. The PacBio sub-reads (length < 1 kb) were removed. To improve the accuracy of the genome sequence, the GATK[4] and the SOAP (SOAP2, SOAPsnp, SOAPindel) tool packages were used to make single-base corrections. To confirm the presence of any plasmid, the filtered Illumina reads were mapped using the SOAP to the bacterial plasmid database[5]. The gene prediction was performed by the glimmer 3[6] with hidden Markov models. The open reading frames (ORFs) were annotated by the Rapid Annotation using Subsystem Technology (RAST) server online (Overbeek et al., 2014). The Clusters of Orthologous Groups (COG) database

was used for general function annotation. For the identification of secondary metabolism gene clusters, the antiSMASH 5.0 program was used (Blin et al., 2019). Whole Genome Shotgun project of *Streptomyces* sp. HM190 has been deposited at DDBJ/ENA/GenBank under the accession CP047318.

Fermentation, Extraction, and Isolation of Strain HM190

Strain HM190 was inoculated into a 1000-mL flask containing 250 mL of the seed culture medium consisting of glucose (0.4%), yeast extract (0.4%), malt extract (1.0%), and $CaCO_3$ (0.2%), with a pH of 7.2. After incubated at 30°C for 3 days on a rotary shaker operating at 250 r/min, the 5.0% seed culture broth was added to a 50 L fermenter (containing 30 L of fermentation medium) incubation for 7 days at 30°C. The fermentation medium component was the same as the isolation medium of MB (marine broth 2216 medium).

The final 30 L of fermentation broth was centrifuged to separate supernatant and bottomed mycelial cake. The mycelial cake was subsequently extracted with MeOH (3 L). The supernatant passed through a Diaion HP-20 resin column (Mitsubushi Chemical Co., Ltd., Tokyo, Japan) and eluted with 95% EtOH. The MeOH extract and the EtOH eluent were concentrated under reduced pressure at 55°C to yield a crude extract (30 g). The crude extract was chromatographed on a silica gel column (Qingdao Haiyang Chemical Group, Qingdao, China; 200-300 mesh) eluted with $CHCl_3$/MeOH (100:0, 98:2, 95:5, 90:10, 80:20, 70:30, 60:40, and 50:50, v/v) to give six fractions (Fr.1–6) based on the TLC profiles. After the Fr.5 was concentrated under reduced pressure at 53°C and dried *in vacuo*, the material was subjected to a Sephadex LH-20 gel column (GE Healthcare, Glies, United Kingdom) and eluted with $CHCl_3$/MeOH (1:1, v/v), to yield two fractions (Fr.5-1 and Fr.5-2) by using TLC detection. The Fr.5-1 was further chromatographed on a silica gel column and eluted with $CHCl_3$/MeOH (100:0, 98:2, 95:5, 90:10, 85:15, 80:20, 75:25, and 70:30 v/v) to give four fractions (Fr.5-1-1–Fr.5-1-4). The Fr.5-1-1 was analyzed and purified by semi-preparative reversed-phase HPLC and eluted with CH_3CN/H_2O (60:40, v/v) to get compound **1** (t_R

28.5 min, 15.2 mg). The Fr.5-1-3 was subjected to a Sephadex LH-20 column eluted with $CHCl_3/MeOH$ (1:1, v/v) to give three fractions (Fr.5-1-3a, Fr.5-1-3b, and Fr.5-1-3c). The Fr.5-1-3c was further separated by semi-preparative reversed-phase HPLC and eluted with CH_3CN/H_2O (48:52, v/v) to get compounds **2** (t_R 37.0 min, 9.8 mg) and **3** (t_R 45.0 min, 5.8 mg), respectively.

Compound **1**: white powder; $[\alpha]_D^{25} = -4$ (c 0.05, EtOH); IR (KBr) ν_{max} 3441.9, 2931.3, 1701.1, 1647.0, 1419.2, 1392.8, and 1287.2 cm^{-1}; UV (EtOH) λ_{max} (log ε) 202 (3.93), 217 (3.82) nm;

^{1}H (400 MHz) and ^{13}C NMR (100 MHz) data shown in **Table 1**; positive HRESIMS m/z 765.4359 [M + Na]$^+$, (calcd. for $C_{39}H_{66}NaO_{13}$, 765.4396).

Compound **2**: white powder; $[\alpha]_D^{25} = -6$ (c 0.05, EtOH); IR (KBr) ν_{max} 3440, 2900, 1700, 1640, 1450, 1380, 1260, 1180, 1080, and 980 cm^{-1}; UV (MeOH) λ_{max} 223 nm (ε 8,900); ^{1}H (400 MHz) and ^{13}C NMR (100 MHz) data shown in **Table 1**; positive HRESIMS m/z 763.4546 [M + Na]$^+$, (calcd. for $C_{39}H_{66}NaO_{13}$, 763.4603).

TABLE 1 | The ^{1}H and ^{13}C NMR data for compounds **1–3** (δ in ppm).

Position	1[a] (in CDCl$_3$)		2[a] (in CDCl$_3$)		3[b] (in CD$_3$OD)	
	δ_C	δ_H (J in Hz)	δ_C	δ_H (J in Hz)	δ_C	δ_H (J in Hz)
1	164.9, C		165.1, C		166.9, C	
2	119.5, CH	6.16 d (15.6)	119.5, CH	6.14 d (15.6)	120.0, CH	6.04 d (15.6)
3	149.9, CH	6.85 d (15.6)	151.1, CH	6.82 d (15.6)	153.8, CH	6.96 d (15.6)
4	75.1, C		75.5, C		76.8, C	
5	79.3, CH	3.82 s	80.1, CH	3.79 br s	81.2, CH	3.75 d (11.8)
6	35.3, CH	1.62 m	39.5, CH	1.52 m	39.6, CH	1.60 m
7	77.2, CH	3.97 br s	77.7, CH	4.04 br m	77.8, CH	4.01 m
8	65.9, CH	3.90 m	35.1, CH$_2$	1.27 m, 1.59 m	36.2, CH$_2$	1.45 m, 1.55 m
9	73.0, CH	2.93 br s	78.4, CH	3.45 br s	78.4, CH	3.26 dd (1.9, 11.3)
10	77.1, C		75.3, C		75.7, C	
11	36.8, CH$_2$	1.27 m	37.5, CH$_2$	1.21 m	38.7, CH$_2$	1.33 m
12	21.9, CH$_2$	1.45 m, 1.59 m	22.5, CH$_2$	1.46 m, 1.66 m	23.8, CH$_2$	1.33 m, 1.68 m
13	32.4, CH$_2$	1.93 m, 2.43 br d (14.0)	32.9, CH$_2$	1.96 m, 2.38 m	35.3, CH$_2$	1.96 m, 2.42 m
14	132.5, CH	5.20 m	132.1, CH	5.23 m	126.2, CH	5.34 m
15	132.7, CH	5.40 m	133.0, CH	5.38 m	129.7, CH	6.35 d (15.4)
16	51.1, CH	1.98 m	50.9, CH	1.99 m	110.0, C	
17	96.9, C		97.1, C		148.8, C	
18	39.7, CH$_2$	1.29 br d (13.6), 2.20 t (13.4)	39.7, CH$_2$	1.33 m, 2.15 t (13.4)	32.8, CH$_2$	2.18 m, 2.90 t (12.4)
19	66.1, CH	4.27 br d (12.0)	66.4, CH	4.25 m	68.9, CH	4.15 ddd (1.8, 4.3, 11.4)
20	34.3, CH	2.10 m	34.7, CH	2.00 m	34.2, CH	1.96 m
21	69.5, CH	5.30 m	69.2, CH	5.36 m	71.9, CH	5.26 m
22	35.3, CH$_2$	1.62 m, 1.80 m	35.4, CH$_2$	1.72 m, 1.84 m	36.8, CH$_2$	1.67 m, 1.73 m
23	98.2, C		98.4, C		99.4, C	
24	34.2, CH$_2$	1.46 m, 1.70 m	29.2, CH$_2$	1.52 m, 1.69 m	30.7, CH$_2$	1.47 m, 1.70 m
25	19.3, CH$_2$	1.68 m	27.0, CH$_2$	1.56 m, 1.93 m	27.8, CH$_2$	1.42 m, 2.16 m
26	30.8, CH$_2$	1.72 m	30.8, CH	1.62 m	32.3, CH	1.60 m
27	72.3, CH	3.97 br s	67.5, CH	3.96 br d (11.6)	69.8, CH	4.02 m
28	43.7, CH$_2$	1.41 m, 1.57 m	41.6, CH$_2$	1.20 m, 1.63 m	41.8, CH$_2$	1.32 m, 1.63 m
29	68.3, CH	3.91 m	68.6, CH	3.86 m	71.4, CH	3.73 m
30	29.9, CH$_2$	1.46 m, 1.60 m	30.3, CH$_2$	1.25 m, 1.52 m	32.1, CH$_2$	1.60 m
31	10.2, CH$_3$	0.98 t (7.2)	10.4, CH$_3$	1.00 t (7.4)	10.5, CH$_3$	0.99 t (6.8)
32	66.2, CH$_2$	3.57 br d (8.0)	66.3, CH$_2$	3.57 m	72.4, CH$_2$	3.44 d (9.8), 3.99 m
33	30.5, CH	1.30 m	30.6, CH	1.48 m	28.6, CH	1.94 m
34	33.7, CH$_2$	1.41 m	34.3, CH$_2$	1.41 m	30.8, CH$_2$	1.29 m, 2.33 dd (5.6, 16.3)
35	28.1, CH$_3$	1.38 s	27.4, CH$_3$	1.40 s	27.4, CH$_3$	1.34 s
36	5.6, CH$_3$	0.92 d (6.8)	5.2, CH$_3$	0.94 t (6.6)	6.0, CH$_3$	0.95 t (6.4)
37	22.4, CH$_3$	1.22 s	19.9, CH$_3$	1.11 s	20.9, CH$_3$	1.04 s
38	6.4, CH$_3$	0.76 d (6.8)	6.3, CH$_3$	0.72 d (7.2)	5.6, CH$_3$	0.8 d (6.8)
39	16.9, CH$_3$	0.79 d (6.4)	11.4, CH$_3$	0.94 d (6.6)	11.7, CH$_3$	0.95 t (6.4)
40			17.1, CH$_3$	0.79 d (6.8)	17.6, CH$_3$	0.99 t (6.8)

^{a} ^{1}H (400 MHz), ^{13}C (100 MHz); ^{b} ^{1}H (600 MHz), ^{13}C (150 MHz).

Compound **3**: white powder; [α] = −5 (c 0.05, EtOH); IR (KBr) ν_{max} 3450, 2950, 1720, 1660, 1460, 1390, 1280, 1180, 1100, 980 cm^{-1}; UV (MeOH) λ_{max} 247 nm (ε 13,500); ^{1}H (600 MHz) and ^{13}C NMR (150 MHz) data shown in **Table 1**; positive HRESIMS m/z 745.4437 [M + Na]$^+$, (calcd. for $C_{39}H_{66}NaO_{13}$, 745.4497). The IR and UV data of compounds **2** and **3** from Akira H. et al.

X-Ray Crystallography

Small seed crystals of compound **1** were produced by controlling evaporation of solutions at room temperature over 2 weeks in CHCl$_3$/MeOH (60:40, v/v). Re-crystallization at 4°C to induce the production of high-quality crystals for X-ray diffraction was conducted for 20 days. A suitable crystal was selected and mounted on a Bruker D8 Venture diffractometer. The crystal was kept at 170.02 K during data collection. The structure was solved with the ShelXT (Sheldrick, 2015) structure solution program using Intrinsic Phasing. Calculations were made with the ShelXL (Kratzert et al., 2015) refinement package using least squares minimization as implementation in Olex2 (Dolomanov et al., 2009). Crystallographic data (excluding structure factor) for compound **1** has been deposited with the Cambridge Crystallographic Data Center under the deposition number CCDC 1990958.

Biological Assay

The antimicrobial activities of compounds **1–3** against pathogenic bacteria *Klebsiella pneumoniae*, methicillin-resistant *Staphylococcus aureus*, and pathogenic fungus *Candida albicans* were detected with the minimum inhibitory concentrations (MICs) method recommended by the Clinical and Laboratory Standards Institute (Wang et al., 2019). Amphotericin B (an antifungal antibiotic) and gentamicin (an antibacterial antibiotic) were used as a positive control.
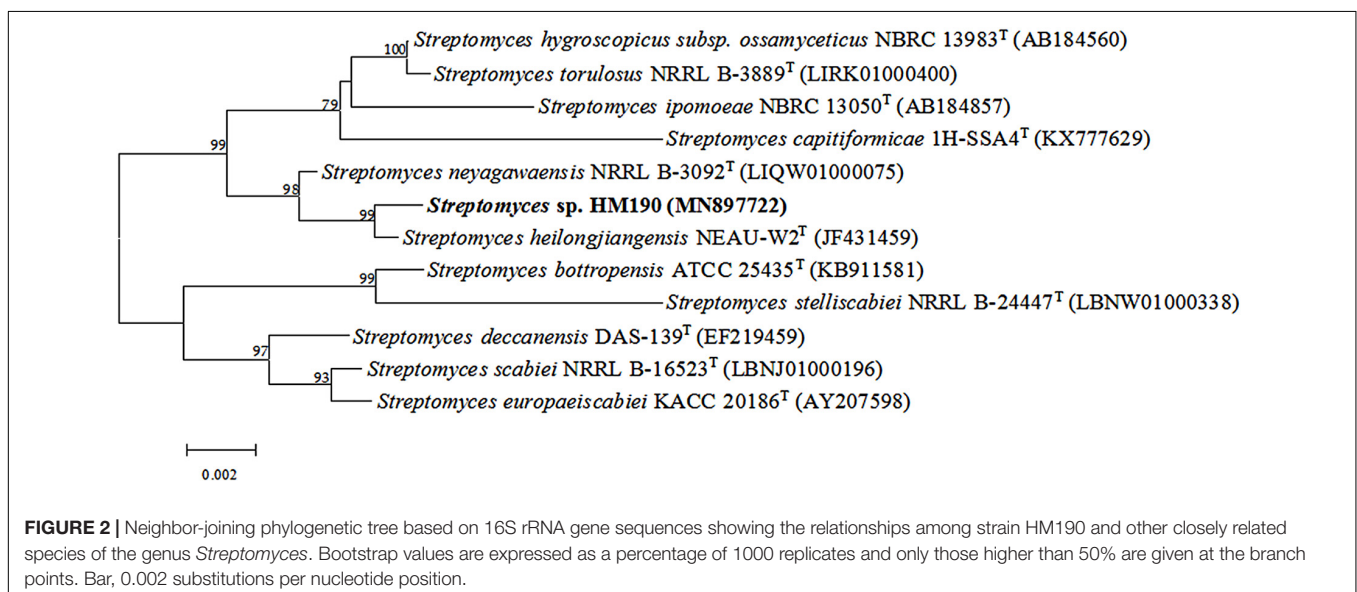
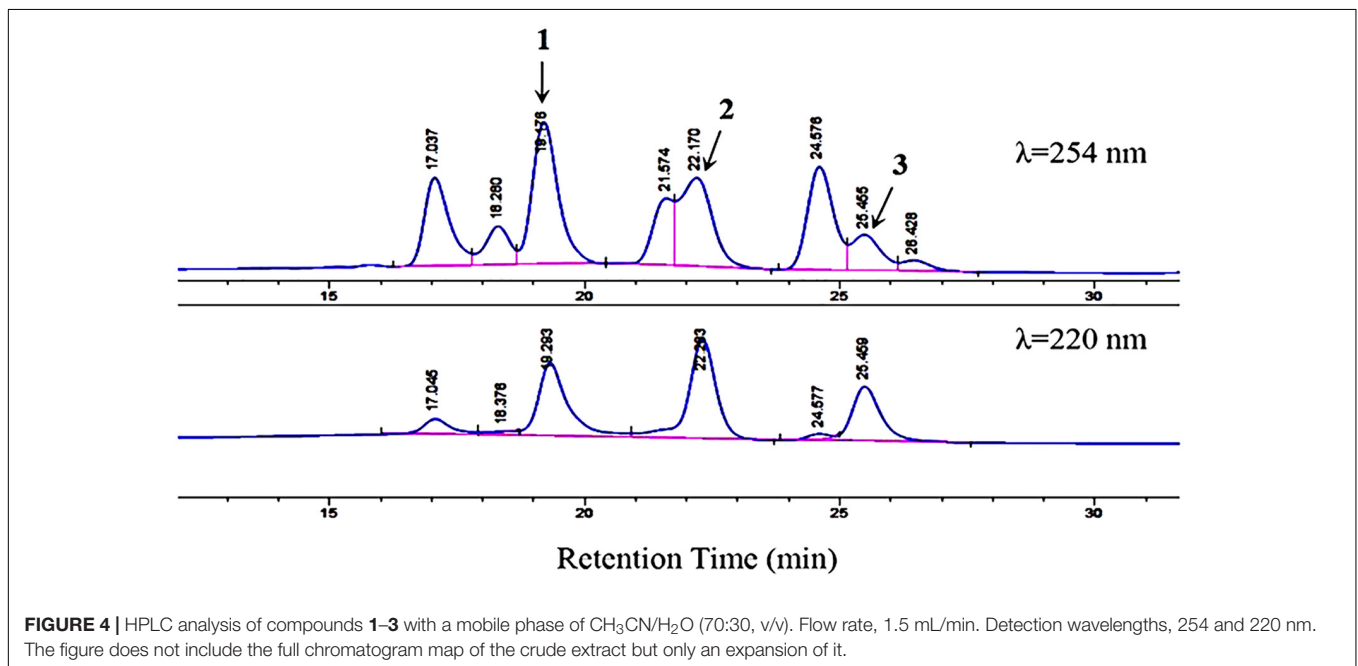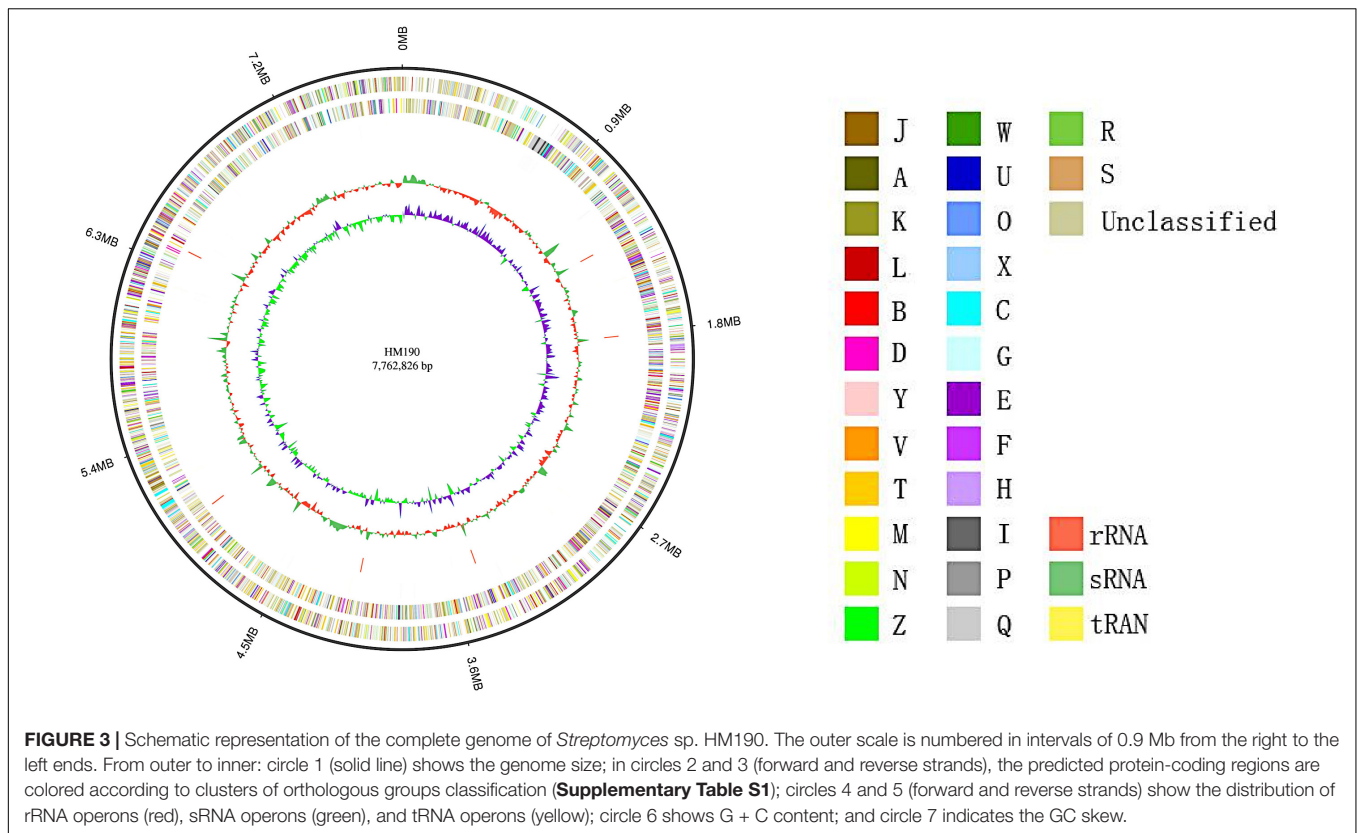The cytotoxic activities of compounds **1–3** were investigated against the human colon tumor cell line HCT116, the human lung carcinoma cell line A549, and the hepatocellular carcinoma cell line HepG2 *in vitro* by the CCK8 (cell counting kit-8) colorimetric method. The cell lines were incubated in a 5% CO$_2$ incubator at 37°C for 4 h under Dulbecco's Modified Eagle's Medium (DMEM) solution containing 10% calf serum. The adherent cells of the logarithmic growth stage were digested and seeded in a 96-well culture plate at a density of 1×10^4 cells per/well. Then the test samples and controls [Frame1] were added to the medium and cultivated for 48 h. Further the CCK8 (Dojindo, Kumamoto, Japan) reagent was added to the medium and cultured for 3 h. Cell viability was detected by the absorbance at 450 nm using a SpectraMax M5 microplate reader (Molecular Devices Inc., Sunnyvale, CA, United States) (Wang et al., 2009). Doxorubicin was used as a positive control. Cell solution (dimethylsulfoxide) was tested as a negative control. The inhibitory rate of cell proliferation was expressed as IC$_{50}$ value.

RESULTS AND DISCUSSION

16S rRNA Gene Sequence and Phylogenetic Analysis

PCR was used to determine the 16S rRNA gene sequence (1451 bp, NCBI GenBank accession number: MN897722) of strain HM190. The results of the analysis indicated that the isolate belonged to the genus *Streptomyces* and showed the highest sequence similarities to *Streptomyces heilongjiangensis* NEAU-W2^T (99.79%) and *Streptomyces neyagawaensis* NRRL B-3092^T (99.59%). In the phylogenetic analysis based on a neighbor-joining tree (**Figure 2**), strain HM190 fell within the cluster of the genus *Streptomyces* and formed a coherent clade with *S. heilongjiangensis* NEAU-W2^T. The clade had firm bootstrap support and represented an independent lineage. Similar results were obtained by using the maximum-parsimony and maximum-likelihood trees (**Supplementary Figures S26, S27**).

FIGURE 2 | Neighbor-joining phylogenetic tree based on 16S rRNA gene sequences showing the relationships among strain HM190 and other closely related species of the genus *Streptomyces*. Bootstrap values are expressed as a percentage of 1000 replicates and only those higher than 50% are given at the branch points. Bar, 0.002 substitutions per nucleotide position.

FIGURE 3 | Schematic representation of the complete genome of *Streptomyces* sp. HM190. The outer scale is numbered in intervals of 0.9 Mb from the right to the left ends. From outer to inner: circle 1 (solid line) shows the genome size; in circles 2 and 3 (forward and reverse strands), the predicted protein-coding regions are colored according to clusters of orthologous groups classification (**Supplementary Table S1**); circles 4 and 5 (forward and reverse strands) show the distribution of rRNA operons (red), sRNA operons (green), and tRNA operons (yellow); circle 6 shows G + C content; and circle 7 indicates the GC skew.

FIGURE 4 | HPLC analysis of compounds **1–3** with a mobile phase of CH_3CN/H_2O (70:30, v/v). Flow rate, 1.5 mL/min. Detection wavelengths, 254 and 220 nm. The figure does not include the full chromatogram map of the crude extract but only an expansion of it.

Genome Sequence and AntiSMASH Analysis

The whole genome sequence of *Streptomyces* sp. HM190 was assembled using the PacBio RSII and Illumina HiSeq400 platforms. High-quality clean data of size 1266 Mb with a total genome size of 9.10 Mb were generated and assembled into a linear chromosome. The complete genome consisted of 776,2826 bp composing a linear chromosome with 71.97% G + C content. No plasmid was identified. A total of 6971 protein-coding genes were predicted. Of these, 4728 genes

(67.8%) were annotated by querying the COG database. A map of the chromosome and the COG functional categories of strain HM190 are shown in **Figure 3**. For further accurate secondary metabolism BGC (SMBGC) mining analysis, 30 SMBGCs of strain HM190 were proposed using antiSMASH 5.0 (Blin et al., 2019), occupying 15.4% of the chromosome (**Supplementary Table S2**).

Twelve of the 30 BGCs were predicted to be responsible for the production of PKS and non-ribosome peptide- (NRPS) derived secondary metabolites, including one type I PKS (cluster 5), one type II PKS (cluster 14), two type III PKS (clusters 2, 16), two NRPS (clusters 3, 21), and six hybrid BGCs (clusters 1, 4, 6, 10, 15, 23), which possessed genes encoding more than one type of biosynthetic enzyme. Cluster 5 encoded for a type I PKS that is probably responsible for the biosynthesis of a

20/21-membered macrolide of apoptolidin. A sequence similarity of 74.5% was obtained between cluster 5 and the *Nocardiopsis* sp. FU 40 apoptolidin gene cluster (NCBI accession number: JF819834) based on BLASTN analysis. According to Du et al. (2011), the apoptolidin gene cluster of *Nocardiopsis* sp. FU 40 produces 10 apoptolidin and isoapoptolidin compounds, and the biosynthetic pathway was confirmed. Cluster 14 was probably involved in the production of a hiroshidine-like compound, based on its high similarity to the type II PKS enzyme from the hiroshidine BGC from *Streptomyces hiroshimensis* (Moon et al., 2019). Gene clusters 2 and 16 encoded, respectively, for type III PKSs that resembled the alkylresorcinol and germicidin PKSs from *Streptomyces* spp. (Funabashi et al., 2008; Becerril et al., 2018). Cluster 3 encoded for an NRPS that probably synthesized scabichelin (Kodani et al., 2013). Cluster 21 was
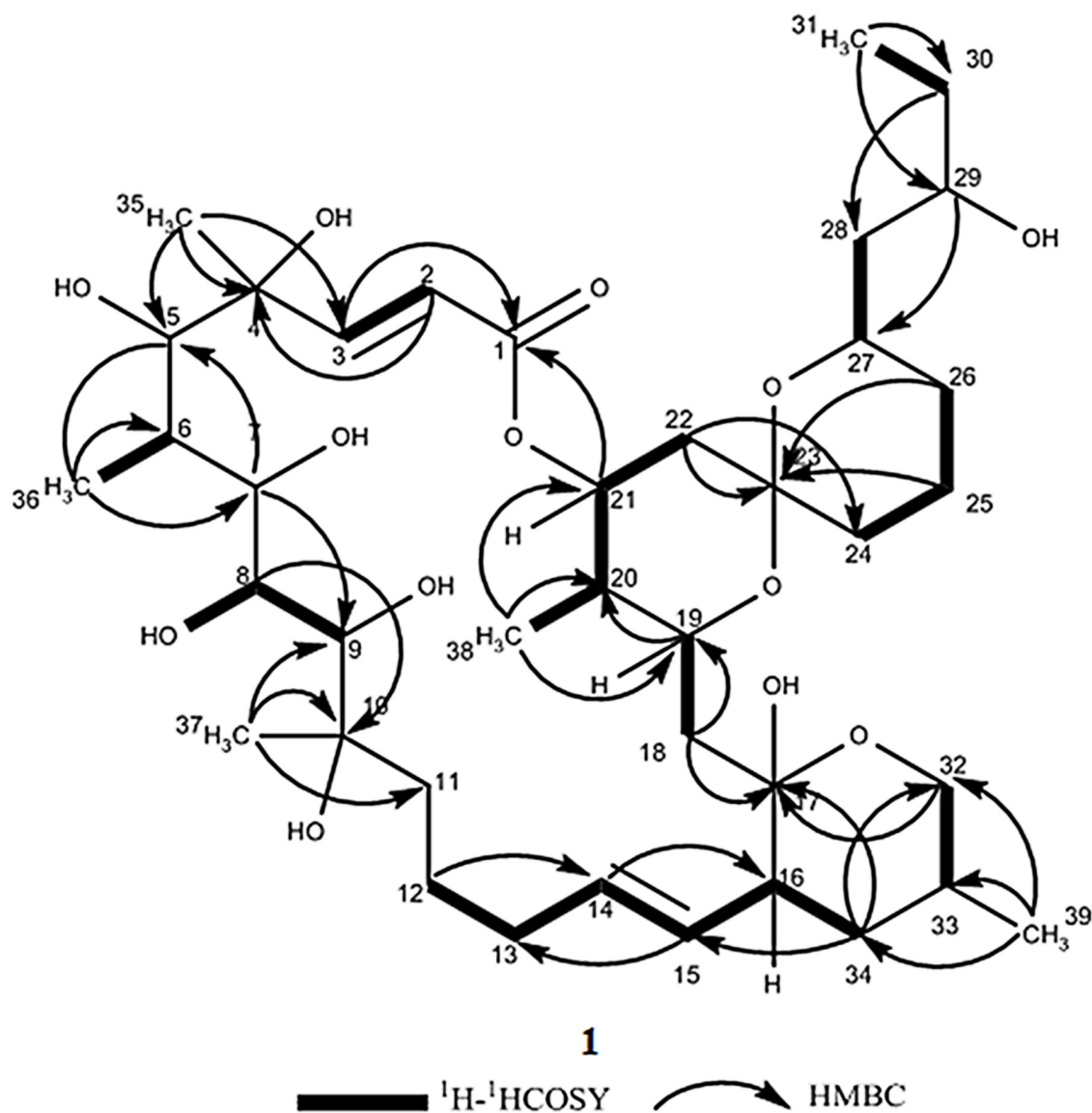

FIGURE 5 | The key ^{1}H-^{1}H COSY and HMBC correlations for compound **1**.

similar to the *Salinispora tropica* CNB-440 gene cluster associated with biosynthesis of the anticancer agent salinosporamide A (Fenical et al., 2009). Based on its high similarity to the recently discovered naphthyridinomycin BGC from *Streptomyces lusitanus*, cluster 1 was probably involved in the production of a naphthyridinomycin-like compound (Pu et al., 2013). Gene clusters 4 and 15 were predicted to be responsible for biosynthesis of gaudimycin- and glycosyl ester-type compounds, respectively (Kallio et al., 2008; Wang et al., 2015). Cluster 6 encoded for a type II PKS that probably synthesized granaticin (Ichinose et al., 1998). Cluster 10 encoded for a *2H*-furan type PKS based on its high similarity to the *Streptomyces* sp. 88-682 gene cluster (Sun et al., 2009). Six gene clusters (8, 9, 11, 20, 22, 29) within the genome of strain HM190 were observed related to saccharide biosynthesis; cluster 11 also harbored genes encoding for melanin formation. Several other secondary metabolites were potentially produced by strain HM190, including two siderophore molecules encoded by clusters 12 and 27 (cluster 12 showed high similarity to desferrioxamine B biosynthetic genes). Bacteriocin or other unspecified ribosomally synthesized and post-translationally modified peptides were encoded by clusters 13 and 25 (cluster 13 showed high similarity to bottromycin A2 biosynthetic genes), cluster 7 (ectoine), cluster 17 (lanthipeptide or lasso peptide), cluster 18 (indole), cluster 19 (halogenide), cluster 28 [linear azol(in)e-containing peptide], and clusters 24, 26, and 30 (terpenes).

Structure Elucidation

Based on the COG categorization of the genome of strain HM190, there were a considerable number of genes related to secondary metabolite biosynthesis, transport, and catabolism (**Figure 3**). Together with the antiSMASH analysis, strain HM190 appeared to be an isolate with prolific potential for the production of various new and unique secondary metabolites. In order to assess this, the strain was grown for scale-up culture in 30 L of fermentation medium for 7 days at 30°C. Results of HPLC analysis of the crude extract are shown in **Figure 4**. Compounds **1–3** were purified and subjected to detailed structural analysis.

Compound **1** was obtained as a white powder with a molecular formula of $C_{39}H_{66}O_{13}$ (seven degrees of unsaturation) based on high-resolution electrospray ionization mass spectroscopy (HRESIMS) data (m/z 765.4359 $[M + Na]^+$, calcd. 765.4396). The ^1H and ^{13}C NMR (**Table 1**), distortionless enhancement by polarization transfer (DEPT) and heteronuclear single quantum coherence (HSQC) spectra for **1** indicated the presence of two double bonds (δ_C 149.9, 119.5, 132.5, and 132.7); five quaternary carbons (δ_C 164.9, 98.2, 96.9, 77.1, and 75.1), including one carbonyl carbon (δ_C 164.9); six methyl groups (δ_C 28.1, 22.4, 16.9, 10.2, 6.4, and 5.6); 12 methylene groups, one of which was oxygenated (δ_C 66.2); and 16 methine groups, eight of which were oxygenated. Detailed analysis of the ^1H–^1H COSY (homonuclear chemical shift correlation spectroscopy) and heteronuclear multiple bond correlation (HMBC) spectra revealed that **1** was a spiroketal 22-membered macrolide with a dihydropyran moiety (**Figure 5**). The spiroketal ring system was established based on the HMBC correlations of H-22 with C-23, of H-22 with C-24, of H-25 with C-23, and of H-26 with C-23, together with the

^1H-^1H COSY correlations of H-21 with H-22, H-24 with H-25, and H-25 with H-26. The HMBC correlations from H-32 to C-17, from H-34 to C-17 and C-32, from H-34 to C-15, and from H-39 to C-32, C-33, and C-34 revealed the presence of a dihydropyran moiety and the fusion of this dihydropyran moiety to the 22-membered macrolide system. This result was supported by the ^1H-^1H COSY correlations H-16/H-34 and H-32/H-33. From these unambiguous one- and two-dimensional correlation NMR spectral data, the structure of **1** was assigned (**Figure 1**) and determined to represent a new 22-membered macrolide. These data were similar to those of phthoramycin, which was previously isolated from *Streptomyces* sp. WK-1875 (Nakagawa et al., 1989). Compound **1** had six methyl groups, whereas phthoramycin contained seven methyl groups. Comparisons of the NMR data between **1** and phthoramycin indicated that **1** differed from phthoramycin by the absence of a methyl substituent at C-26 and the presence of a hydroxy group at C-8.

The molecular formula of compound **2** was established as $C_{40}H_{68}O_{12}$ (seven degrees of unsaturation) by the HRESIMS data (m/z 763.4546 $[M + Na]^+$, calcd. 763.4603). The molecular formula of compound **2** revealed that it had the same weight as the known kaimonolide A (Akira et al., 1989). Based on detailed NMR data analysis, the structure of compound **2** was found to show the same planar structure with kaimonolide A. Compound **3** was isolated as an analog of compound **2**. The molecular formula of compound **3** was established as $C_{40}H_{66}O_{11}$ (eight degrees of unsaturation) from the HRESIMS data (m/z 745.4437 $[M + Na]^+$, calcd. 745.4497). The ^1H and ^{13}C NMR

TABLE 2 | Crystal data and structural refinement for compound **1**.

Empirical formula	$C_{39}H_{66}O_{13}$
Formula weight	742.91
Temperature (K)	170.02
Crystal system	Monoclinic
Space group	P21
Unit cell dimensions	a = 9.9665(11) Å, α = 90°
	b = 21.014(2) Å, β = 96.321(3)
	c = 21.950(2) Å, γ = 90°
Volume (Å³)	4569.3(8)
Z	4
Calculated density (Mg/m³)	1.080
Absorption coefficient (mm⁻¹)	0.422
F(000)	1616.0
Crystal size (mm³)	0.06 × 0.06 × 0.05
Wavelength (Å)	1.34139
Theta range for data collection	7.32–109.99°
Index ranges	−12 ≤ h ≤ 12, −25 ≤ k ≤ 25, -26 ≤ l ≤ 25
Reflections collected	42,745
Independent reflections	17,092 [R(int) = 0.0883, R(sigma) = 0.1157]
Data/restraints/parameters	17,092/18/964
Goodness-of-fit on F²	0.997
Final R indices [I ≥ 2sigma(I)]	R_1 = 0.0656, wR_2 = 0.1426
Final R indices [all data]	R_1 = 0.1294, wR_2 = 0.1700
Largest diff. peak and hole (e Å⁻³)	0.23 and −0.25
Flack parameter	−0.11(15)

spectral data for **2** and **3** are shown in **Table 1**. Comparisons of the molecular formulas and NMR data of **2** and **3** indicated that **3** was a dehydrated product of **2**, resulting from the formation of a double bond at C-16/C-17. It should be noted that during our studies, compound **2** would have gradually changed to **3** in $CDCl_3$ solution (Akira et al., 1989). Compounds **2** and **3** also closely resembled phthoramycin and cytovaricin B, which have been reported in *Streptomyces* spp. (Sakurai et al., 1983; Nakagawa et al., 1989).

Absolute Configurations of Compounds 1–3

To define the correct absolute configuration of compound **1**, a single crystal of compound **1** was prepared for X-ray single-crystal diffraction. Crystals of compound **1** ($C_{39}H_{66}O_{13}$,

CCDC 1990958) were almost colorless and monoclinic with typical dimensions $0.06 \times 0.06 \times 0.05$ mm^3. Compound **1** crystallized in space group P21 with unit cell parameters a = 9.9665(11), b = 21.014(2), c = 21.950(2) Å, and Z = 4 molecules per unit cell. The refined structure of compound **1** had final R index [I ≥ 2sigma(I)] values of $R_1 = 0.0656$, $wR_2 = 0.1426$, and final R index [all data] values of $R_1 = 0.1294$, $wR_2 = 0.1700$. Detailed crystal data and structure refinements are shown in **Table 2**. The quality of the crystal was high enough for absolute configuration analysis to be carried out (Palmer and Potter, 2008). The absolute structure Flack parameter was −0.11(15), which was equal to 0.0 with standard deviation of 15 (Flack, 1983), confirming that the structure of **1** had been assigned the correct absolute configuration. **Figure 6** shows the ORTEP diagram of compound **1** according to the X-ray data.

FIGURE 6 | The ORTEP diagram of compound **1** obtained from X-ray data.
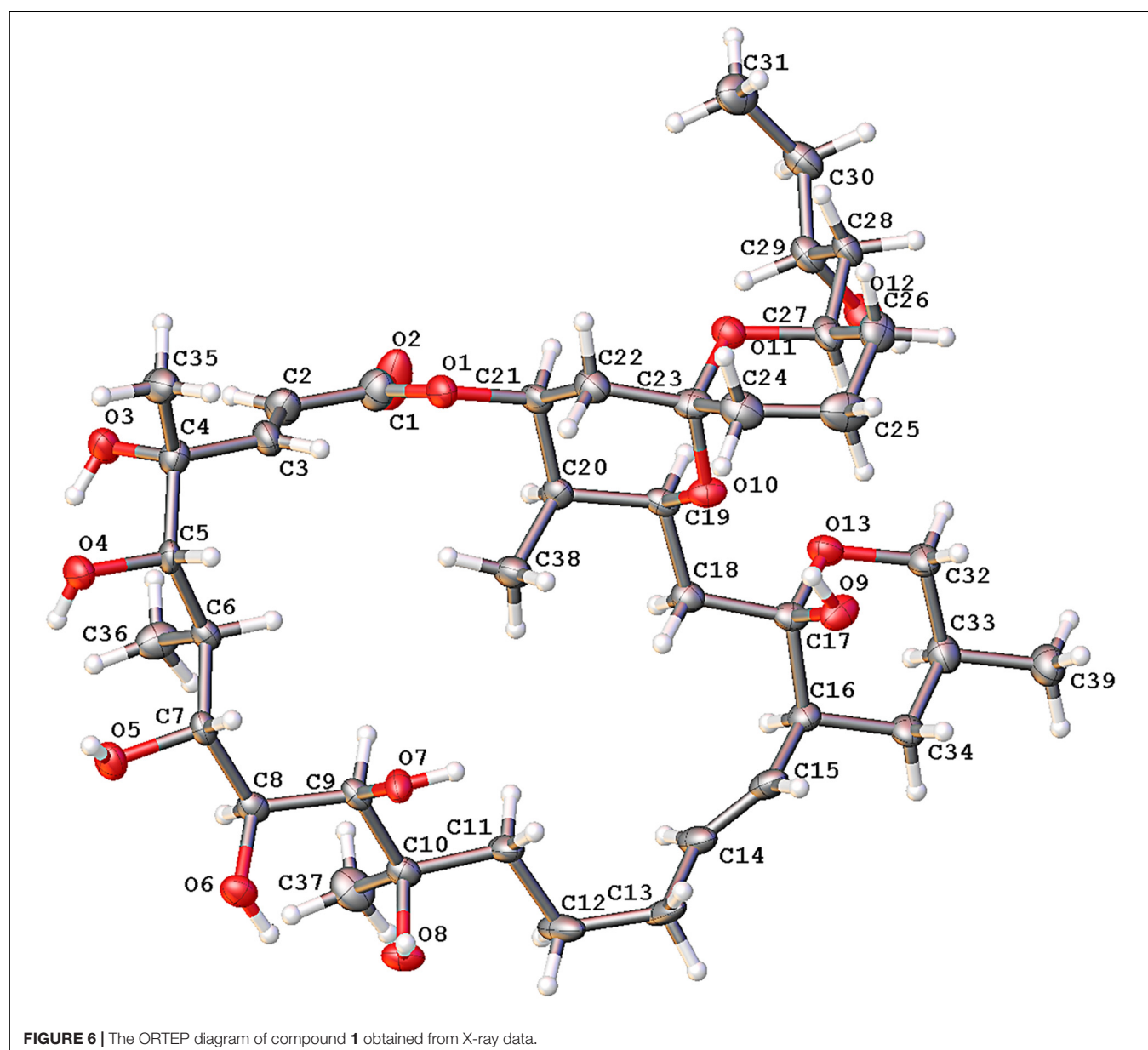
Compound **2** was dehydrated at C16/C-17 to produce compound **3**. Thus, we determined the absolute configurations of compounds **2** and **3** simultaneously. Based on the similarity of the NMR spectra of compounds **1**–**3**, including chemical shifts and peak multiplicities (**Table 1**), the multiple stereocenters of **2** and **3** had the same absolute configuration as in compound **1**, although within differences at C-26 and C-27, because of the addition of a methyl substituent at C-26. According to Bilyk et al. in 2019, the absolute configurations of 22- to 26-membered macrolides compounds were confirmed by the data of NMR spectra, single-crystal X-ray crystallography, and elegant total synthesis of representative. Detailed NMR data comparison revealed a striking structural similarity of compounds **2**, **3** to kaimonolide A (Akira et al., 1989; Bilyk et al., 2019) and cytovaricin B (Sakurai et al., 1983; Yamashita et al., 1997). Finally, the absolute configurations of compounds **2** and **3** were established as shown in **Figure 1**.

Biosynthetic Pathway Analysis

In strain HM190, the predicted BGC of macrolide compounds **1**–**3** contained 15 individual ORFs, including eight type I PKS genes, three cytochrome P450 genes, one crotonyl-CoA reductase (CCR) gene, one transcriptional regulator gene, and two hypothetical protein genes (Du et al., 2011; Bilyk et al., 2019). PKS genes S1–S8 were proposed to be responsible for the biosynthesis of the polyketide core of compounds **1**–**3**. A suggested module and domain organization and a proposed model for the PKS template assembly of the macrolide backbone are shown in **Figure 7**. PKS gene S2 encoded the putative protein possessing the probable initiating module. The next 13 extension modules were proposed to be encoded by genes S3–S8 and were ordered according to the predicted linear arrangement of the required domains. Finally, the terminating module protein was identified to be encoded by gene S8 by its terminal punctuation with a thioesterase domain. One additional PKS gene S1 containing a complete module sequence "KS-AT-KR-ER-DH-ACP" and CCR apparently encoded a free-standing isobutylmalonyl-ACP that assembled to the macrolide backbone of module 7 in gene S5. After the core skeletons were constructed, the structural diversity of both macrocyclization and spiroketalization was mainly due to the tailoring reactions of cytochrome P450 genes to complete the hydroxylation reactions.
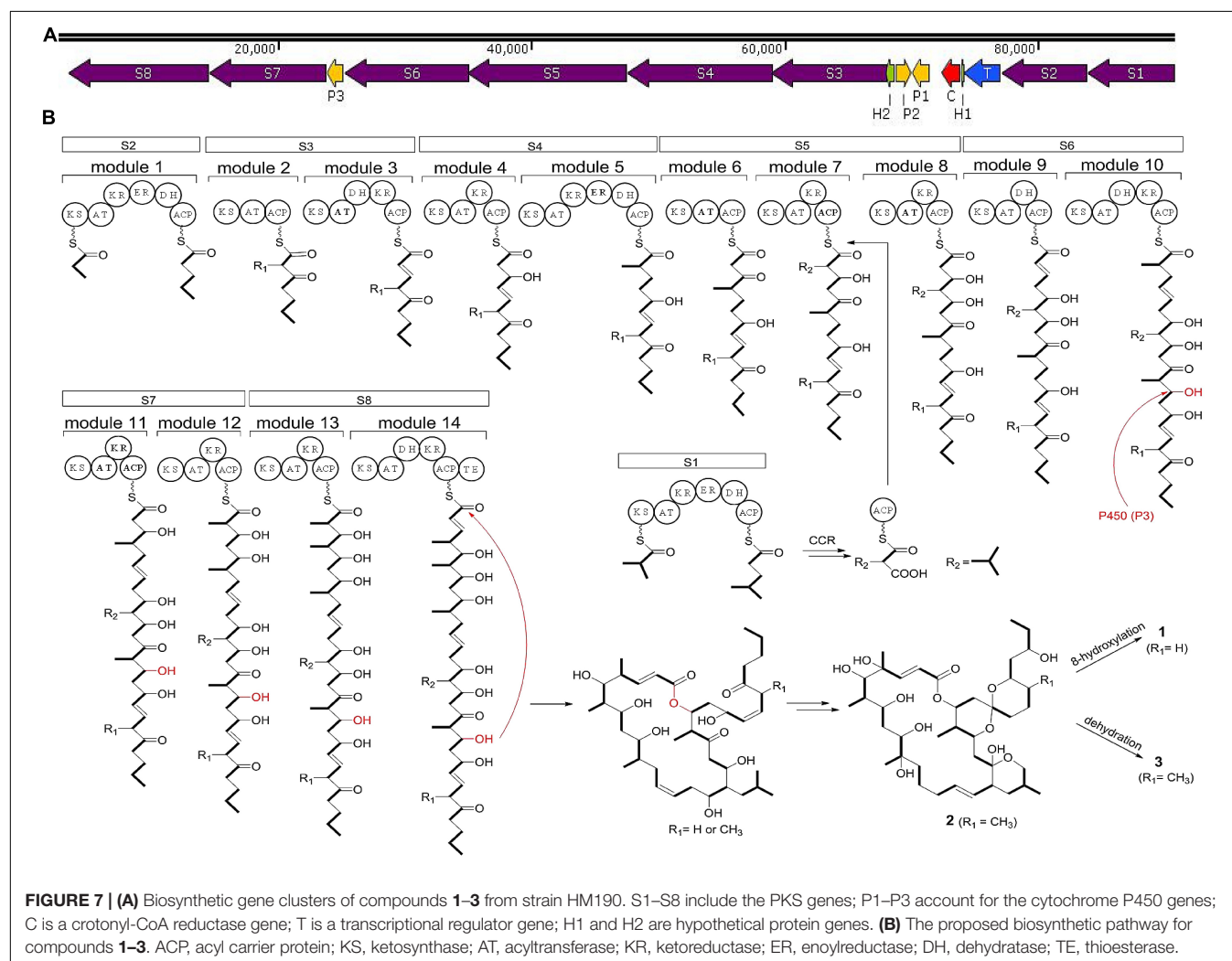

FIGURE 7 | (A) Biosynthetic gene clusters of compounds **1**–**3** from strain HM190. S1–S8 include the PKS genes; P1–P3 account for the cytochrome P450 genes; C is a crotonyl-CoA reductase gene; T is a transcriptional regulator gene; H1 and H2 are hypothetical protein genes. **(B)** The proposed biosynthetic pathway for compounds **1**–**3**. ACP, acyl carrier protein; KS, ketosynthase; AT, acyltransferase; KR, ketoreductase; ER, enoylreductase; DH, dehydratase; TE, thioesterase.

TABLE 3 | Cytotoxic activities of compounds **1–3** against selected human tumor cell lines.

Compound	IC_{50} (μg/mL)		
	HepG2	A549	HCT116
1	8.76	15.97	22.13
2	10.52	19.63	28.25
3	12.69	20.17	29.70
Doxorubicin	0.90	0.95	1.04

Biological Activities

The cytotoxic activities of compounds **1–3** against HepG2, A549, and HCT116 human tumor cell lines are shown in **Table 3**. All the compounds suppressed the proliferation of the tested cells but exhibited different levels of activity. Compound **1** showed stronger cytotoxic activities than compounds **2** and **3**, with a half maximal inhibitory concentration value (IC_{50}) of 8.76 μg/mL against hepatocellular carcinoma cell line HepG2, with IC_{50} of 15.97 μg/mL against lung carcinoma cell line A549, and with IC_{50} of 22.13 μg/mL against colon tumor cell line HCT116.

The antibacterial and antifungal activities of the three compounds were detected against three human pathogens: Gram-positive bacterium methicillin-resistant *S. aureus*, Gram-negative bacterium *K. pneumoniae*, and fungus *C. albicans*. The MICs of compounds **1–3** were found to be >10 mg/mL, indicating that the three compounds had no biological activities against the tested pathogens.

CONCLUSION

During a study of microorganism diversity in mangrove samples, a white-pigmented colony was picked and named HM190. Detailed 16S rRNA gene sequencing and phylogenetic analysis identified the strain as *Streptomyces*. The whole-genome sequence of strain HM190 was obtained using the PacBio RSII and the Illumina HiSeq 4000 platforms by long-read single-molecule real-time sequencing technology. The assembled genome comprised a linear chromosome as a single contig of 7,762,826 bp with 71.97% G + C content. Based on the results of antiSMASH analysis, a total of 30 gene clusters were predicted to be involved in the biosynthesis of secondary metabolites; 12 of the 30 BGCs were responsible for the production of PKS- and NRPS-derived secondary metabolites. Several other secondary metabolites were also predicted by their BGCs. Gene cluster 5 was predicted to be involved in the production of an apoptolidin-like macrolide based on its high similarity of 74.5% to the type I PKS enzyme from the macrolide BGC of *Nocardiopsis* sp. FU 40 (Du et al., 2011). Furthermore, a chemical investigation was carried out on strain HM190, which led to the isolation of three 22-membered macrolides (compounds **1–3**). The structures of the three compounds were determined based on the HRESIMS and NMR data. The absolute configurations of compounds **1–3** were established by the X-ray single-crystal diffraction and NMR data analysis. All three compounds showed moderate cytotoxic activities against hepatocellular carcinoma cell line HepG2, human lung carcinoma cell line A549, and human colon tumor cell line HCT116. A biosynthetic pathway for the three compounds was proposed on basis of the PKS gene cluster analysis.

DATA AVAILABILITY STATEMENT

The datasets generated for this study can be found in the GenBank/EMBL/DDBJ and accession number for the 16S rRNA gene sequence of strain HM190 is MN897722. Whole Genome Shotgun project of *Streptomyces* sp. HM190 has been deposited at DDBJ/ENA/GenBank under the accession CP047318.

ETHICS STATEMENT

All studies of this article were processed with the standard of biosecurity and institutional safety procedures.

AUTHOR CONTRIBUTIONS

YY conducted and performed the experiments and prepared the manuscript. JW and MW designed the experiments. XM and SW determined the compounds structures and the biosynthetic pathway analysis. NA performed the biological activities experiments. ZZ and RZ undertook the genome analysis. CY and YN performed the microbiology experiments. JZ revised the manuscript. All authors contributed to the article and approved the submitted version.

FUNDING

ACKNOWLEDGMENTS

SUPPLEMENTARY MATERIAL

The Supplementary Material for this article can be found online at: https://www.frontiersin.org/articles/10.3389/fmicb.2020.01464/full#supplementary-material

The following are available online: the HRESIMS and NMR spectra (**Supplementary Figures S1–S25**) of compounds **1–3**, the maximum-parsimony and maximum-likelihood phylogenetic trees (**Supplementary Figures S26, S27**) of strain HM190, the cluster of orthologous groups (COG) classification (**Supplementary Table S1**) and the antiSMASH-predicted BGCs (**Supplementary Table S2**) of strain HM190, and the crystal data (**Supplementary Tables S3–S5**) of compound **1**.

REFERENCES

Akira, H., Hideki, O., Toshitaka, K., Mitsuru, N., Hiroshi, H., and Akira, I. (1989). Structure of kaimonolide A, a novel macrolide plant growth inhibitor from a *Streptomyces* strain. *Agr. Biol. Chem.* 53, 2831–2833. doi: 10.1271/bbb1961.53.2831

Alfredo, B., Sarmiento, V. A., Miguel, O., Pérez, V. I., Martín, J., Nuria, D. P., et al. (2017). Lobophorin K, a new natural product with cytotoxic activity produced by *Streptomyces* sp. M-207 associated with the deep-sea coral *Lophelia pertusa*. *Mar. Drugs* 15:144. doi: 10.3390/md15050144

Altschul, S. F., Madden, T. L., Schaffer, A. A., Zhang, J., and Lipman, D. J. (1997). Gapped BLAST and PSI-BLAST: a new generation of protein database search programs. *Nucleic Acids Res.* 25, 3389–3402. doi: 10.1093/nar/25.17.3389

Anzai, Y., Kim, H., Park, J. Y., Wakabayashi, H., and Oyaizu, H. (2000). Phylogenetic affiliation of the *Pseudomonads* based on 16s rRNA sequence. *Int. J. Syst. Evol. Microbiol.* 50, 1563–1589. doi: 10.1099/00207713-50-4-1563

Becerril, A., Alvarez, S., Brana, A. F., Rico, S., Diaz, M., Santamaria, R. I., et al. (2018). Uncovering production of specialized metabolites by *Streptomyces argillaceus*: activation of cryptic biosynthesis gene clusters using nutritional and genetic approaches. *PLoS One* 13:e0198145. doi: 10.1371/journal.pone.0198145

Bentley, S. D., Chater, K. F., Cerdeño-Tárraga, A. M., Challis, G. L., Thomson, N. R., James, K. D., et al. (2002). Complete genome sequence of the model actinomycete *Streptomyces coelicolor* A3(2). *Nature* 417, 141–147. doi: 10.1038/417141a

Bilyk, O., Samborskyy, M., and Leadlay, P. F. (2019). The biosynthetic pathway to ossamycin, a macrocyclic polyketide bearing a spiroacetal moiety. *PLoS One* 14:e0215958. doi: 10.1371/journal.pone.0215958

Blin, K., Shaw, S., Steinke, K., Villebro, R., Ziemert, N., Lee, S. Y., et al. (2019). AntiSMASH 5.0: updates to the secondary metabolite genome mining pipeline. *Nucleic Acids Res.* 47, 81–87. doi: 10.1093/nar/gkz310

Blunt, J. W., Copp, B. R., Keyzers, R. A., Munro, M. H. G., and Michèle, R. P. (2015). Marine natural products. *Nat. Prod. Rep.* 32, 116–211. doi: 10.1039/C4NP00144C

Dolomanov, O. V., Bourhis, L. J., Gildea, R. J., Howard, J. A. K., and Puschmann, H. (2009). Olex2: a complete structure solution, refinement and analysis program. *J. Appl. Crystallogr.* 42, 339–341. doi: 10.1107/S0021889808042726

Du, Y., Derewacz, D. K., Deguire, S. M., Teske, J., and Bachmann, B. O. (2011). Biosynthesis of the apoptolidins in *Nocardiopsis* sp, Fu 40. *Tetrahedron* 67, 6568–6575. doi: 10.1016/j.tet.2011.05.106

Felsenstein, J. (1981). Evolutionary trees from DNA sequences: a maximum likelihood approach. *J. Mol. Evol.* 17, 368–376. doi: 10.1007/BF01734359

Fenical, W., Jensen, P. R., Palladino, M. A., Lam, K. S., Lloyd, G. K., and Potts, B. C. (2009). Discovery and development of the anticancer agent salinosporamide A (npi-0052). *Bioorgan. Med. Chem.* 17, 2175–2180. doi: 10.1016/j.bmc.2008.10.075

Flack, H. D. (1983). On enantiomorph-polarity estimation. *Acta Crystallogr.* 39, 876–881. doi: 10.1107/S0108767300101762

Funabashi, M., Funa, N., and Horinouchi, S. (2008). Phenolic lipids synthesized by type III polyketide synthase confer penicillin resistance on *Streptomyces griseus*. *J. Biol. Chem.* 283, 13983–13991. doi: 10.1074/jbc.M710461200

Girão, M., Ribeiro, I., Ribeiro, T., Azevedo, I. C., Pereira, F., Urbatzka, R., et al. (2019). *Actinobacteria* isolated from *Laminaria ochroleuca*: a source of new bioactive compounds. *Front. Microbiol.* 10:683. doi: 10.3389/fmicb.2019.00683

Holguin, G., Vazquez, P., and Bashan, Y. (2001). The role of sediment microorganisms in the productivity, conservation, and rehabilitation of mangrove ecosystems: an overview. *Biol. Fert. Soils* 33, 265–278. doi: 10.1007/s003740000319

Huang, X., Zhou, S., Huang, D., Chen, J., and Zhu, W. (2016). *Streptomyces spongiicola* sp. nov. an actinomycete derived from marine sponge. *Int. J. Syst. Evol. Microbiol.* 66, 738–743. doi: 10.1099/ijsem.0.000782

Hwang, K. S., Kim, H. U., Charusanti, P., Palsson, B. Ø., and Lee, S. Y. (2014). Systems biology and biotechnology of *Streptomyces* species for the production of secondary metabolites. *Biotechnol. Adv.* 32, 255–268. doi: 10.1016/j.biotechadv.2013.10.008

Ichinose, K., Bedford, D. J., Tornus, D., Bechthold, A., and Hopwood, D. A. (1998). The granaticin biosynthetic gene cluster of *Streptomyces violaceoruber* TU22: sequence analysis and expression in a heterologous host. *Cell Chem. Biol.* 5, 647–659. doi: 10.1016/S1074-5521(98)90292-7

Ioanna, P., Konstantinos, L., Jakob, J., Chen, I. A., Tatyana, S., Bahador, N., et al. (2012). The genomes online database (GOLD) v. 4: status of genomic and metagenomic projects and their associated metadata. *Nucleic Acids Res.* 40, 571–579. doi: 10.1093/nar/gkr1100

Kallio, P., Liu, Z., Mäntsälä, P., Niemi, J., and Metsä-Ketelä, M. (2008). Sequential action of two flavoenzymes, PGAe and PGAm, in angucycline biosynthesis: chemoenzymatic synthesis of gaudimycin C. *Chem. Biol.* 15, 157–166. doi: 10.1016/j.chembiol.2007.12.011

Kathiresan, K., and Bingham, B. L. (2001). Biology of mangroves and mangrove ecosystems. *Adv. Mar. Biol.* 40, 81–251. doi: 10.1016/S0065-2881(01)40003-4

Kimura, M. (1981). A simple method for estimating evolutionary rates of base substitutions through comparative studies of nucleotide sequences. *J. Mol. Evol.* 16, 111–120. doi: 10.1007/BF01731581

Kodani, S., Bicz, J., Song, L., Deeth, R. J., Ohnishi-Kameyama, M., Yoshida, M., et al. (2013). Structure and biosynthesis of scabichelin, a novel tris-hydroxamate siderophore produced by the plant pathogen *Streptomyces scabies* 87.22. *Org. Biomol. Chem.* 11, 4686–4694. doi: 10.1039/C3OB40536B

Kratzert, D., Holstein, J. J., and Krossing, I. (2015). DSR: enhanced modelling and refinement of disordered structures with Shelxl. *J. Appl. Crystallogr.* 48, 933–938. doi: 10.1107/S1600576715005580

Li, M., Hong, Y. G., Cao, H. L., and Gu, J. D. (2011). Mangrove trees affect the community structure and distribution of anammox bacteria at an anthropogenic-polluted mangrove in the pearl river delta reflected by 16s rRNA and hydrazine oxidoreductase (hzo) encoding gene analyses. *Ecotoxicology* 20, 1780–1790. doi: 10.1007/s10646-011-0711-4

Liu, R., Deng, Z., and Liu, T. (2018). *Streptomyces* species: ideal chassis for natural product discovery and overproduction. *Metab. Eng.* 50, 74–84. doi: 10.1016/j.ymben.2018.05.015

Moon, K., Xu, F., Zhang, C., and Seyedsayamdost, M. R. (2019). Bioactivity-HiTES unveils cryptic antibiotics encoded in actinomycete bacteria. *ACS Chem. Biol.* 14, 767–774. doi: 10.1021/acschembio.9b00049

Nakagawa, A., Miura, S., Imai, H., Imamura, N., and Omura, S. (1989). Structure and biosynthesis of a new antifungal antibiotic, phthoramycin. *J. Antibiot.* 42, 1324–1327. doi: 10.7164/antibiotics.42.1324

Overbeek, R., Olson, R., Pusch, G. D., Olsen, G. J., Davis, J. J., Disz, T., et al. (2014). The SEED and the Rapid Annotation of microbial genomes using subsystems technology (RAST). *Nucleic Acids Res.* 42, 206–214.

Palmer, R. A., and Potter, B. S. (2008). X-ray structures and absolute configurations of the antibiotics oligomycins A, B and C: inhibitors of ATP synthase. *J. Chem. Crystallogr.* 38, 243–253. doi: 10.1007/s10870-008-9317-y

Pu, J. Y., Peng, C., Tang, M. C., Zhang, Y., Guo, J. P., Song, L. Q., et al. (2013). Naphthyridinomycin biosynthesis revealing the use of leader peptide to guide nonribosomal peptide assembly. *Org. Lett.* 15, 3674–3677. doi: 10.1021/ol401549y

Rzhetsky, A., and Nei, M. (1992). Statistical properties of the ordinary least-squares, generalized least-squares, and minimum-evolution methods of phylogenetic inference. *J. Mol. Evol.* 35, 367–375. doi: 10.1007/BF00161174

Saitou, N., and Nei, M. (1987). The neighbour-joining method: a new method for reconstructing phylogenetic trees. *J. Mol. Biol. Evol.* 4, 406–425. doi: 10.1093/oxfordjournals.molbev.a040454

Sakurai, T., Kihara, T., and Isono, K. (1983). Structure of cytovaricin–acetonitrile (1:1), $C_{47}H_{80}O_{16} \cdot C_2H_3N$. *Acta Crystallogr.* 39, 295–297. doi: 10.1107/S010827018300445X

Santos, H. F. D., Cury, J. C., Flávia, L. D. C., Santos, A. L. D., Tiedje, J., Elsas, J. D. V., et al. (2011). Mangrove bacterial diversity and the impact of oil contamination revealed by pyrosequencing: bacterial proxies for oil pollution. *PLoS One* 6:e16943. doi: 10.1371/journal.pone.0016943

Sheldrick, G. M. (2015). Shelxt integrated space group and crystal structure determination. *Acta Crystallogr.* 71, 3–8. doi: 10.1107/S2053273314026370

Studholme, D. J. (2016). Genome update. Let the consumer beware: *Streptomyces* genome sequence quality. *Microb. Biotechnol.* 9, 3–7. doi: 10.1111/1751-7915.12344

Sun, Y., Hahn, F., Demydchuk, Y., Chettle, J., Tosin, M., Osada, H., et al. (2009). In vitro reconstruction of tetronate RK-682 biosynthesis. *Nat. Chem. Biol.* 6, 99–101. doi: 10.1038/nchembio.285

Tamura, K., Peterson, D., Peterson, N., Stecher, G., Nei, M., and Kumar, S. (2011). MEGA 5: molecular evolutionary genetics analysis using maximum likelihood, evolutionary distance, and maximum parsimony methods. *J. Mol. Biol. Evol.* 28, 2731–2739. doi: 10.1093/molbev/msr121

Thatoi, H., Behera, B. C., Mishra, R. R., and Dutta, S. K. (2013). Biodiversity and biotechnological potential of microorganisms from mangrove ecosystems: a review. *Ann. Microbiol.* 63, 1–19. doi: 10.1007/s13213-012-0442-7

Thompson, J. D., Higgins, D. G., and Gibson, T. J. (1994). CLUSTAL W: improving the sensitivity of progressive multiple sequence alignment through sequence weighting, positions-specific gap penalties and weight matrix choice. *Nucleic Acids Res.* 22, 4673–4680. doi: 10.1093/nar/22.22.4673

Tian, Y., Liu, H. J., Zheng, T. L., Kwon, K. K., Kim, S. J., and Yan, C. L. (2008). PAHs contamination and bacterial communities in mangrove surface sediments of the jiulong river estuary. *China. Mar. Pollut. Bull.* 57, 707–715. doi: 10.1016/j.marpolbul.2008.03.011

Waksman, S. A., and Henrici, A. T. (1943). The nomenclature and classification of the actinomycetes. *J. Bacteriol.* 46, 337–341. doi: 10.1002/path.1700560116

Wang, J. D., Zhang, H., Ying, L. P., Wang, C. X., Jiang, N., Zhou, Y., et al. (2009). Five new epothilone metabolites from *Sorangium cellulosum* strain So0157-2. *J. Antibiot.* 62, 483–487. doi: 10.1038/ja.2009.55

Wang, R. J., Zhang, S. Y., Ye, Y. H., Yu, Z., Qi, H., Zhang, H., et al. (2019). Three new isoflavonoid glycosides from the mangrove-derived actinomycete *Micromonospora aurantiaca* 110B. *Mar. Drugs* 17:294. doi: 10.3390/md17050294

Wang, X., Reynolds, A. R., Elshahawi, S. I., Shaaban, K. A., and Thorson, J. S. (2015). Terfestatins B and C, new p-terphenyl glycosides produced by *Streptomyces* sp. RM-5–8. *Org. Lett.* 17, 2796–2799. doi: 10.1021/acs.orglett.5b01203

Xu, J. (2011). Biomolecules produced by mangrove-associated microbes. *Curr. Med. Chem.* 18, 5224–5266. doi: 10.2174/092986711798184307

Xu, L., Ye, K. X., Dai, W. H., Sun, C., Xu, L. H., and Han, B. N. (2019). Comparative genomic insights into secondary metabolism biosynthetic gene cluster distributions of marine Streptomyces. *Mar. Drugs* 17:498. doi: 10.3390/md17090498

Yamashita, N., Shin-Ya, K., Kitamura, M., Wakao, H., Furihata, K., Furihata, K., et al. (1997). Cytovaricin B, a new inhibitor of JAK-STAT signal transduction produced by *Streptomyces torulosus*. *J. Antibiot.* 50, 440–442. doi: 10.7164/antibiotics.50.440

Yan, L. L., Han, N. N., Zhang, Y. Q., Yu, L. Y., Chen, J., Wei, Y. Z., et al. (2010). Antimycin A18 produced by an endophytic *Streptomyces albidoflavus* isolated from a mangrove plant. *J. Antibiot.* 63, 259–261. doi: 10.1038/ja.2010.21

Ye, Y., Chen, C., Ren, Y., Wang, R., Zhang, C., Han, S., et al. (2019). *Pseudomonas mangrovi* sp. nov., isolated from mangrove soil. *Int. J. Syst. Evol. Microbiol.* 69, 377–383. doi: 10.1099/ijsem.0.003141

Yoon, S. H., Ha, S. M., Kwon, S., Lim, J., and Chun, J. (2017). Introducing EzBioCloud: a taxonomically united database of 16S rRNA gene sequences and whole-genome assemblies. *Int. J. Syst. Evol. Microbiol.* 67, 1613–1617. doi: 10.1099/ijsem.0.001755

Zhao, X. Q., Li, W. J., Jiao, W. C., Li, Y., Yuan, W. J., Zhang, Y. Q., et al. (2009). *Streptomyces xinghaiensis* sp. nov. isolated from marine sediment. *Int. J. Syst. Evol. Microbiol.* 59, 2870–2874. doi: 10.1099/ijs.0.009878-0

Zhong, X., Tian, Y., Niu, G., and Tan, H. (2013). Assembly and features of secondary metabolite biosynthetic gene clusters in *Streptomyces ansochromogenes*. *Sci. China Life Sci.* 56, 609–618. doi: 10.1007/s11427-013-4506-0

Zhu, H., Jiang, S., Yao, Q., Wang, Y., Chen, M., Chen, Y., et al. (2011). *Streptomyces fenghuangensis* sp. nov. isolated from seawater. *Int. J. Syst. Evol. Microbiol.* 61, 2811–2815. doi: 10.1099/ijs.0.029280-0

Conflict of Interest: JZ was employed by AstraZeneca Trading Co., Ltd.

The remaining authors declare that the research was conducted in the absence of any commercial or financial relationships that could be construed as a potential conflict of interest.